Bioorganic & Medicinal Chemistry Letters xxx (xxxx) xxx–xxx

Contents lists available at ScienceDirect

Bioorganic & Medicinal Chemistry Letters

journal homepage: www.elsevier.com/locate/bmcl

Muscarinic agonist, (±)-quinuclidin-3-yl-(4-fluorophenethyl)(phenyl) carbamate: High affinity, but low subtype selectivity for human M_1 – M_5 muscarinic acetylcholine receptors

Na-Ra Lee[a], Satheesh Gujarathi[b], Shobanbabu Bommagani[b], Kiranbabu Siripurapu[a], Guangrong Zheng[b], Linda P. Dwoskin[a,*]

[a] Department of Pharmaceutical Sciences, College of Pharmacy, University of Kentucky, Lexington, KY 40536, United States
[b] Department of Pharmaceutical Sciences, College of Pharmacy, University of Arkansas for Medical Sciences, Little Rock, AR 72205, United States

ARTICLE INFO

Keywords:
Carbamate
Muscarinic acetylcholine receptors
[^{3}H]N-methylscopolamine binding
[^{3}H]dopamine release
Substance use disorders
Chronic obstructive pulmonary disease

ABSTRACT

Novel quinuclidinyl *N*-phenylcarbamate analogs were synthesized, and binding affinities at M_1-M_5 muscarinic acetylcholine receptor (mAChR) subtypes were determined using Chinese hamster ovary (CHO) cell membranes stably expressing one specific subtype of human mAChR. Although not subtype selective, the lead analog (±)-quinuclidin-3-yl-(4-fluorophenethyl)(phenyl)carbamate (**3c**) exhibited the highest affinity (K_i = 2.0, 13, 2.6, 2.2, 1.8 nM) at each of the M_1-M_5 mAChRs, respectively. Based on results from the [^{3}H]dopamine release assay using rat striatal slices, **3c** acted as an agonist at mAChRs. The effect of **3c** was inhibited by the non-selective mAChR antagonist, scopolamine, and **3c** augmented release evoked by oxotremorine. A potent analog from the same scaffold, (±)-quinuclidin-3-yl-(4-methoxyphenethyl)(phenyl)-carbamate (**3b**) exhibited the greatest selectivity (17-fold) at M_3 over M_2 mAChRs. These analogs could serve as leads for further discovery of novel subtype-selective muscarinic ligands with the goal of providing therapeutics for substance use disorders and chronic obstructive pulmonary disease.

Muscarinic acetylcholine receptors (mAChRs) consist of five subtypes (M_1, M_2, M_3, M_4 and M_5 mAChRs). Each mAChR subtype has a unique expression pattern and activates distinct cholinergic signaling mechanisms and cellular functions.[1,2] Each mAChR subtype can be considered as a therapeutic target for relevant diseases that are associated with specific cell functions modulated by the mAChR subtype. For example, M_1 mAChRs expressed in cerebral cortex, striatum and hippocampus mediate learning and memory processes.[3] M_1 mAChRs allosteric agonists, VU0357017 and VU0364572, enhance spatial learning in rats in the Morris water maze.[4,5] Agonists at M_1 mAChRs have been proposed as pharmacotherapeutics for Alzheimer's disease and schizophrenia.[1,6,7] Another example is the M_3 mAChR, which mediates contraction of smooth muscles in the respiratory system.[8,9] M_3 mAChR antagonists, such as tiotropium or umeclidinium have been approved by the US Food and Drug Administration (FDA) as therapeutics for chronic obstructive pulmonary disease (COPD).[1,10,11] More recently, a combination therapy including umeclidinium and vilanterol, a β2-adrenergic agonist, was approved by the FDA for COPD.[12] Thus, mAChRs are viable targets for drug discovery.

M_5 mAChRs are specifically and highly expressed in the ventral tegmental area (VTA), a brain region containing dopamine (DA) neuronal cell bodies, which project to the nucleus accumbens (NAc).[13–18] Importantly, NAc DA release mediates the rewarding effects of many substances with high abuse liability, including opioids (e.g., morphine) and psychostimulants (e.g., cocaine and amphetamines).[19–22] With respect to opioids, morphine-induced DA release in the NAc is absent in M_5 mAChR knockout (KO) mice, linking M_5 mAChRs to opioid-induced reward.[23] Direct infusion into VTA of a virus containing M_5 mAChR DNA increased both M_5 mAChR expression and morphine-induced locomotor activity compared to control mice, suggesting that M_5 mAChRs mediate DA-related behaviors.[24] Relative to wild-type mice, M_5 mAChR KO mice exhibit a decreased amount of time spent in the cocaine-paired compartment in the conditioned place preference assay[25,26] and decreased cocaine i.v. self-administration,[27] suggesting M_5 mAChRs mediate cocaine reward and reinforcement, respectively.

Since M_5 mAChRs are highly expressed in VTA, micro infusion of nonselective mAChRs antagonists (e.g., scopolamine and atropine) into VTA allows for quasi-selective inhibition of M_5 mAChR function. Scopolamine microinfused unilaterally into VTA decreased morphine-evoked DA release in NAc in mice.[23] Atropine microinfused bilaterally

* Corresponding author.
E-mail address: ldwoskin@uky.edu (L.P. Dwoskin).

https://doi.org/10.1016/j.bmcl.2018.12.022
Received 27 August 2017; Received in revised form 21 November 2018; Accepted 10 December 2018

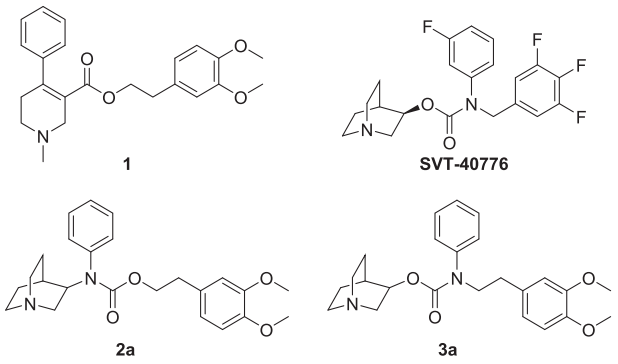

Fig. 1. Structures of compound **1**, SVT-40776, **2a**, and **3a**.

into VTA also decreased morphine-induced hyperlocomotion in mice, supporting a critical role for VTA M_5 mAChRs in modulating opioid effects on behavior.[28] Thus, both pharmacological and genetic approaches to reduce M_5 mAChR function provide consistent results implicating this mAChR subtype in the effects of opioids on DA neurochemistry and related behaviors.

The above findings led us to hypothesize that discovery of selective M_5 mAChRs antagonists may provide novel pharmacotherapeutics that act to decrease the activity of VTA DA projections to NAc, thereby reducing the reinforcing effects of substances with high abuse liability. Previously, we described a 1,2,5,6-tetrahydropyridine-3-carboxylic acid scaffold from which several M_5 mAChRs antagonists were found.[29] From this series of compounds, compound **1** (Fig. 1) exhibited the greatest selectivity (11-fold) at M_5 over M_1 mAChRs; however, **1** provided only modest affinity (K_i = 2.24 μM) for M_5 mAChRs.[29] Compound **1** inhibited oxotremorine-induced DA release from superfused rat striatal slices, revealing an antagonist action at M_5 mAChRs.[29]

The 3,4-dimethoxyphenethyl group in compound **1** was suggested to play an important role in its binding preference at the M_5 subtype.[29] Quinuclidinyl carbamate mAChR antagonists such as SVT-40776 (Fig. 1) and its analogs also have high affinity at mAChRs.[30] In an effort to improve analog affinity and selectivity at M_5 mAChRs, we report herein the synthesis and evaluation of hybrid compounds, **2a** and **3a** (Fig. 1), and a series of related analogs (Tables 1 and 2).

The syntheses of analogs **2–6** are depicted in Schemes 1 and 2. *N*-Phenylquinuclidin-3-amine (**8**) was synthesized as an enantiomeric mixture by reductive amination of quinuclidinone (**7**) with aniline. Conversion of **8** to carbamoyl chloride **9** followed by reaction with appropriate alcohols under microwave irradiation afforded analogs of general structure **2** as enantiomeric mixtures (Scheme 1). *N*-Alkylation of aniline with phenyl ring substituted phenethyl bromide under microwave irradiation afforded compound **10**. Conversion of **10** to carbamoyl chloride **11** followed by reaction with (±)-3-quinuclidinol, (±)-*N*-methylpiperidin-3-ol, *N*-methylpiperidin-4-ol, or tropine under microwave irradiation afforded analogs of general structure **3**, **4**, **5**, and **6**, respectively (Scheme 2).

Initially, affinity at M_5 mAChRs was determined for all analogs. Since M_5 mAChRs have relatively high sequence homology with $M_3 > M_1 > M_4 > M_2$ mAChRs (85%, 79%, 73% and 68%, respectively),[31] we next determined affinity of all analogs at M_3 and M_1 mAChRs. Analogs with high affinity ($K_i \leq 10$ nM) were evaluated also at M_2 and M_4 mAChRs to assess subtype selectivity. Chinese hamster ovary (CHO) cell lines individually expressing each of the human M_1-M_5 mAChRs were generously provided by Dr. Tom Bonner, National Institute of Mental Health. Analog-induced inhibition of [^{3}H]N-methylscopolamine (NMS) binding was used to determine affinity at each of mAChR subtypes.[32,33] Amount of [^{3}H]NMS bound after a 60-min incubation in the absence and presence of a range of analog concentrations was plotted as a function of analog concentration to obtain IC_{50} values. IC_{50} values were used to calculate compound affinity (inhibition constant, K_i) using the Cheng and Prusoff equation.[34] Maximal inhibition (I_{max}) of specific [^{3}H]NMS binding was represented as a percent of control (absence of compound). Atropine was used as the positive control, and its K_i values at M_1, M_2, M_3 and M_5 were 0.44, 0.90, 0.53, and 0.60 nM, respectively, in good agreement with literature values.[35,36]

The K_i and I_{max} values of analogs with general structure **2** at M_1, M_2, M_3, and M_5 mAChRs are provided in Table 1. Compound **2a**, in which the R group is 3,4-dimethoxyphenethyl, is the prototypic analog in this series. Compared with parent compound **1**, **2a** retained affinity at M_5 mAChRs, however, selectivity over other mAChR subtypes was diminished. Substituents on the phenyl ring of the R group and the length between the phenyl ring and *O* atom had important influences on binding affinity. Thus, a wide range of K_i values (19 nM − 6.98 μM) was obtained, whereas the majority of the compounds completely inhibited [^{3}H]NMS binding (I_{max} = 85.9–100% of control). Overall, analogs with a one-carbon linker (**2b**, **2d**, **2j**, **2l**, **2o**, and **2q**) had the highest affinity within each subgroup of compounds having the same substituents on the phenyl ring. However, analogs with a longer linker generally exhibited higher preference for M_5 compared with the corresponding one-carbon linker counterparts. Among the analogs in this series, **2m**, in which the R group is 3,4-dichlorophenethyl, exhibited relatively high affinity (K_i = 80 nM) and the greatest selectivity (4.5-fold) for M_5 over M_1 mAChRs.

Transposition of the phenylalkyl group and the quinuclidin-3-yl group in **2** resulted in analogs **3a**, **3b**, and **3c** as enantiomeric mixtures (Table 2). The design of this group of "rearranged" analogs was based on hypotheses that spatial rearrangement or reorientation of the pharmacophore elements in mAChR ligands would alter affinity and selectivity profiles.[37] Compound **3c** with an *N*-4-fluorophenethyl group exhibited the highest affinity at M_5, M_1 and M_3 mAChRs (K_i = 1.8, 2.0 and 2.6 nM, respectively). Thus, **3c** is ~ 5-fold and 32 to 48-fold, respectively, higher than **3b** having a 3-methoxyphenethyl, and **3a** having a 3,4-dimethoxyphenethyl group. These findings indicate that substituents on the phenyl ring have major impact on affinity and that an electron-withdrawing group may be favorable for receptor binding. Replacement of the quinuclidin-3-yl group in **3** with an *N*-methylpiperidin-3-yl, an *N*-methylpiperidin-4-yl, or a tropan-4-yl provided analogs **4a/b/c**, **5a/b/c**, and **6a/b**, respectively (Table 2). Affinity at M_5, M_1 and M_3 mAChRs for these analogs was lower than their corresponding quinuclidine-containing analogs **3a/b/c**. Despite the overall increase in affinity in this series of analogs compared to analogs in the **2** series, none of these compounds exhibited preference for M_5 mAChRs. Of note, analogs in the **2**, **3**, and **4** series were racemic.

As in our previous studies[29], the lead analog **3c** was evaluated using a functional assay determining inhibition of oxotremorine-induced DA release from superfused rat striatal slices. Oxotremorine is a non-selective agonist at mAChRs.[39] If analog-induced inhibition is observed, then this suggests that the analog acts via an antagonist action at mAChRs. For the [^{3}H]DA release assay, rat striatal slices were incubated with 0.1 μM [^{3}H]DA for 30 min, and then, were superfused with buffer for 60 min to obtain stable efflux of [^{3}H]DA.[29,38] Samples were collected for 15 min to determine basal [^{3}H]DA outflow. Superfusion continued for 35 min in the absence and presence scopolamine (1 and 10 μM, positive control) or **3c** (0.1, 1, and 10 μM) added to the superfusion buffer. Then, oxotremorine (100 μM)[28] was added to the buffer for 25 min. The ability of scopolamine and **3c** to inhibit oxotremorine-evoked [^{3}H]DA overflow was determined. In agreement with our previous findings, oxotremorine increased [^{3}H]DA overflow compared to control, and scopolamine (1 and 10 μM) inhibited (51% and 59%, respectively) oxotremorine-evoked [^{3}H]DA overflow ($[F_{3,35} = 6.13]$, $p < 0.005$, one-way ANOVA followed by Tukey's test; Fig. 2). The results are consistent with the predicted outcome that scopolamine (positive control) inhibits oxotremorine-evoked DA release from rat striatum. The ability of lead compound **3c** to inhibit oxotremorine-evoked [^{3}H]DA overflow from superfused rat striatal

Table 1
Structures and binding affinity at M_1, M_2, M_3, and M_5 mAChRs for atropine and analogs with general structure **2.**[a]

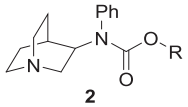

2

Compd	R	[^{3}H]NMS binding K_i ± SEM (μM) (I_{max} ± SEM, % inhibition)				Selectivity	
		M_1	M_2	M_3	M_5	M_1/M_5	M_2/M_3
Atropine	–	0.00044 ± 0.0001[a] (99.5 ± 0.28)	0.0009 ± 0.00005 (99.4 ± 0.74)	0.00053 ± 0.00006 (99.3 ± 0.63)	0.0006 ± 0.00003 (96.7 ± 0.50)	1.7	0.7
1[b]	–	25.3	> 100	> 100	2.24	11	–
2a	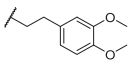	6.98 ± 0.65 (90.6 ± 0.61)	ND[c]	2.76 ± 0.23 (85.9 ± 1.55)[d]	3.49 ± 0.09 (94.0 ± 0.63)	2.0	–
2b	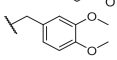	0.77 ± 0.03 (96.8 ± 0.24)	ND	1.02 ± 0.11 (95.4 ± 0.45)	0.55 ± 0.02 (98.7 ± 0.41)	1.4	–
2c	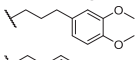	1.46 ± 0.14 (97.1 ± 0.33)	ND	1.56 ± 0.22 (96.3 ± 0.58)	1.61 ± 0.09 (99.0 ± 1.9)	0.9	–
2d		0.19 ± 0.02 (99.5 ± 0.15)	0.12 ± 0.01 (99.4 ± 0.28)	0.09 ± 0.004 (98.6 ± 0.42)	0.15 ± 0.03 (97.2 ± 0.24)	1.3	1.2
2e		0.79 ± 0.08 (88.5 ± 1.37)	ND	0.30 ± 0.01 (99.1 ± 0.504)	0.26 ± 0.03 (96.9 ± 4.4)	3.0	–
2f	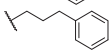	0.78 ± 0.05 (99.1 ± 0.28)	ND	0.55 ± 0.03 (98.9 ± 0.42)	0.26 ± 0.008 (95.7 ± 0.17)	3.0	–
2g	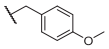	0.71 ± 0.06 (97.9 ± 0.21)	ND	1.15 ± 0.06 (95.7 ± 0.52)	0.47 ± 0.05 (97.1 ± 0.89)	1.5	–
2h	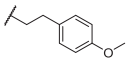	0.76 ± 0.02 (98.4 ± 0.08)	ND	0.42 ± 0.05 (99.3 ± 0.22)	0.23 ± 0.005 (98.9 ± 0.09)	3.3	–
2i	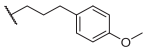	0.59 ± 0.02 (98.5 ± 0.19)	ND	0.39 ± 0.04 (96.8 ± 1.25)	0.64 ± 0.10 (99.5 ± 3.5)	0.9	–
2j	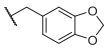	0.03 ± 0.003 (100 ± 0.18)	0.03 ± 0.005 (99.4 ± 0.87)	0.019 ± 0.002 (99.9 ± 0.72)	0.04 ± 0.003 (99.7 ± 0.37)	0.8	1.7
2k	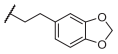	0.63 ± 0.10 (99.6 ± 0.40)	ND	0.29 ± 0.03 (98.0 ± 0.53)	0.24 ± 0.06 (97.1 ± 4.8)	2.6	–
2l	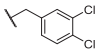	0.06 ± 0.002 (100 ± 0.24)	0.22 ± 0.009 (97.5 ± 1.76)	0.07 ± 0.009 (95.8 ± 0.78)	0.06 ± 0.001 (98.6 ± 4.75)	0.9	3.3
2m	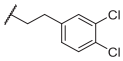	0.37 ± 0.02 (99.9 ± 0.36)	ND	0.26 ± 0.02 (99.8 ± 0.27)	0.08 ± 0.02 (98.8 ± 0.30)	4.5	–
2n	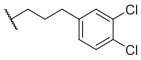	0.17 ± 0.01 (100 ± 0.10)	0.30 ± 0.02 (99.9 ± 0.063)	0.06 ± 0.003 (100 ± 0.25)	0.13 ± 0.003 (99.4 ± 0.30)	1.3	4.7
2o	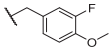	0.07 ± 0.003 (99.5 ± 0.99)	0.10 ± 0.01 (98.8 ± 0.64)	0.05 ± 0.003 (100 ± 0.022)	0.04 ± 0.01 (96.7 ± 0.50)	1.5	1.8
2p	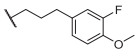	0.43 ± 0.03 (100 ± 0.14)	ND	0.25 ± 0.03 (99.8 ± 1.08)	0.26 ± 0.004 (99.4 ± 0.22)	1.7	
2q		0.04 ± 0.001 (100 ± 0.14)	0.03 ± 0.001 (99.7 ± 0.60)	0.02 ± 0.0003 (99.0 ± 0.56)	0.03 ± 0.003 (97.4 ± 0.13)	1.2	1.3
2r	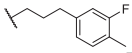	0.20 ± 0.004 (100 ± 0.25)	ND	0.13 ± 0.009 (100 ± 0.29)	0.13 ± 0.004 (99.9 ± 0.45)	1.5	
2s	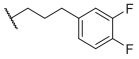	0.30 ± 0.02 (100 ± 0.25)	ND	0.22 ± 0.008 (99.5 ± 1.09)	0.10 ± 0.003 (99.4 ± 0.30)	3.0	–

[a] Three independent experiments, each with duplicate samples, were performed to obtain K_i values (Mean ± SEM).
[b] Data from Ref. [29].
[c] Not determined.
[d] No plateau for the mean inhibition curve was obtained; I_{max} % inhibition at 100 μM analogs was reported.

slices was determined (Fig. 3). Scopolamine (10 μM) was included as a positive control in these experiments. Similar to the results illustrated in Fig. 2, oxotremorine increased [^{3}H]DA overflow and scopolamine decreased the stimulatory effect of oxotremorine. In contrast to expectations, **3c** did not inhibit oxotremorine-evoked [^{3}H]DA overflow, but rather, augmented oxotremorine-evoked [^{3}H]DA overflow. One-way ANOVA followed by Tukey's test revealed that **3c** (10 μM) increased oxotremorine-evoked [^{3}H]DA overflow relative to oxotremorine alone (scopolamine 0 μM; [$F_{3,11} = 6.83$], $p < 0.005$; Fig. 3). Augmentation of the effect of oxotremorine by **3c** suggests that **3c** acts as an agonist at mAChRs.

To further determine if **3c** acts as a mAChR agonist, the ability of scopolamine to inhibit **3c**-evoked [^{3}H]DA overflow was determined. One-way ANOVA followed by Tukey's test revealed that the **3c**-evoked increase in [^{3}H]DA overflow was inhibited by scopolamine (10 μM) ([$F_{5,42} = 6.92$], $p < 0.0001$; Fig. 4). Since the effect of **3c** was inhibited by a nonselective mAChR antagonist, scopolamine, these results support the interpretation that **3c** acts as an agonist at mAChRs to increase [^{3}H]DA overflow from rat striatal slices.

Whereas oxotremorine (1, 10, and 100 μM)-evoked striatal [^{3}H]DA overflow was not altered in M_1 or M_2 mAChR KO mice, oxotremorine-evoked [^{3}H]DA overflow was increased in M_3 KO mice, abolished in M_4

Table 2
Structures and binding affinity at M_1, M_2, M_3, M_4, and M_5 mAChRs for analogs **3-6.**[a]

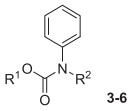

3-6

Compd	R^1	R^2	[^{3}H]NMS binding K_i ± SEM, μM(I_{max} ± SEM, % inhibition)					Selectivity	
			M_1	M_2	M_3	M_4	M_5	M_1/M_5	M_2/M_3
3a		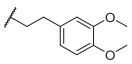	0.095 ± 0.0037 (100 ± 0.14)	0.35 ± 0.02 (98.6 ± 1.57)	0.06 ± 0.006 (99.7 ± 0.91)	ND[b]	0.065 ± 0.002 (99.8 ± 0.56)	1.5	5.7
4a		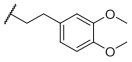	4.30 ± 0.49 (94.3 ± 0.61)	ND	4.36 ± 0.90 (85.6 ± 0.85)[c]	ND	4.49 ± 0.32 (89.2 ± 0.87)	1.0	
5a		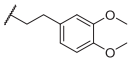	0.77 ± 0.082 (99.0 ± 0.16)	ND	1.28 ± 0.10 (96.6 ± 0.58)	ND	0.38 ± 0.03 (96.5 ± 2.81)	2.0	
6a	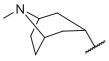	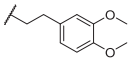	1.87 ± 0.17 (95.3 ± 0.25)	ND	2.80 ± 0.03 (88.8 ± 0.49)[c]	ND	1.37 ± 0.07 (95.9 ± 0.91)	1.4	
3b		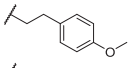	0.01 ± 0.0003 (100 ± 0.16)	0.13 ± 0.025 (99.7 ± 0.48)	0.008 ± 0.0003 (99.9 ± 0.41)	0.025 ± 0.0002 (99.9 ± 0.37)	0.01 ± 0.0005 (100 ± 0.68)	1.0	17.1
4b		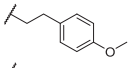	0.69 ± 0.092 (98.6 ± 0.36)	ND	1.32 ± 0.069 (96.2 ± 0.28)	ND	1.05 ± 0.02 (97.7 ± 0.45)	0.7	–
5b		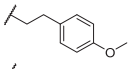	0.28 ± 0.038 (99.8 ± 0.33)		0.57 ± 0.092 (99.7 ± 0.43)	ND	0.19 ± 0.01 (99.7 ± 0.82)	1.5	–
6b	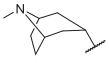	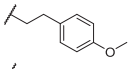	0.35 ± 0.02 (99.7 ± 0.05)	ND	0.27 ± 0.01 (98.9 ± 0.35)	ND	0.24 ± 0.02 (97.9 ± 2.0)	1.5	–
3c		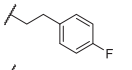	0.002 ± 0.0001 (99.9 ± 0.11)	0.013 ± 0.003 (100 ± 0.71)	0.0026 ± 0.0001 (100 ± 1.39)	0.0022 ± 0.0001 (99.8 ± 0.33)	0.0018 ± 0.0001 (99.8 ± 0.71)	1.1	5.0
4c		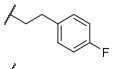	0.12 ± 0.006 (99.9 ± 0.07)	ND	0.35 ± 0.05 (99 ± 1.37)	ND	0.15 ± 0.01 (99.9 ± 1.64)	0.8	–
5c		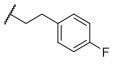	0.07 ± 0.002 (100 ± 0.14)	ND	0.14 ± 0.019 (100 ± 0.50)	ND	0.06 ± 0.002 (100 ± 0.35)	1.2	–

[a] Three independent experiments, each with duplicate samples, were performed to obtain K_i values (Mean ± SEM).
[b] Not determined.
[c] No plateau for the mean inhibition curve was obtained; I_{max} % inhibition at 100 μM analogs was reported.

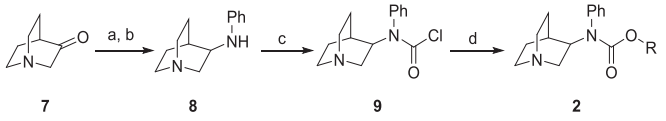

Scheme 1. Reagents and conditions: (a) aniline, EtOH, reflux; (b) $NaBH_4$, EtOH, 95%; (c) triphosgene, Et_3N, CH_2Cl_2, −78 °C, 73%; (d) ROH, KO*t*-Bu, toluene, MWI, 150 °C, 30 min, 28–52%.

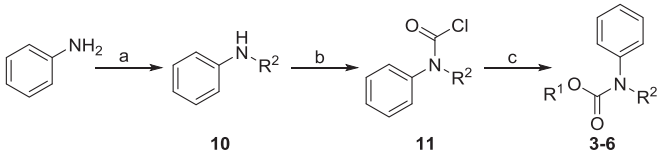

Scheme 2. Reagents and conditions: (a) R^2Br, KI, CH_3CN, MWI, 160 °C, 15 min, 83–99%; (b) triphosgene, Et_3N, CH_2Cl_2, −78 °C, 85–90%; (c) R^1OH, KO*t*-Bu, toluene, MWI, 150 °C, 15 min, 56–82%.

KO mice, and decreased by 50% in M_5 KO mice.[40] Thus, M_1 or M_2 mAChRs do not appear to have a role in mediating striatal DA release in mice. Also, M_3, M_4 and M_5 mAChRs appear to play differing roles in mediating striatal DA release in mice. In contrast to VTA where M_5 mAChR subtype expression predominates, M_3, M_4 and M_5 mAChRs mediate oxotremorine-evoked [^{3}H]DA overflow from striatal slices in mice. If allowed to extrapolate from these results obtained using striatal

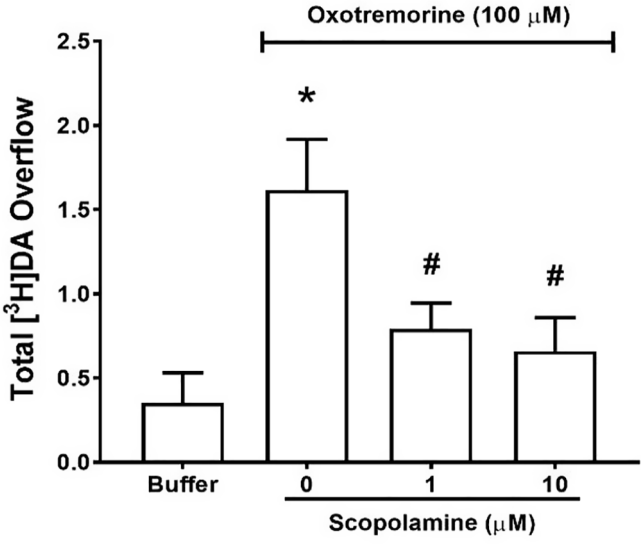

Fig. 2. Scopolamine (1 and 10 μM, positive control) inhibits oxotremorine (100 μM)-evoked [^{3}H]DA overflow from superfused rat striatal slices. Data are presented as mean ± SEM. $^*p < 0.05$ compared to buffer; $^\#p < 0.05$ compared to oxotremorine alone (scopolamine 0 μM), n = 10.

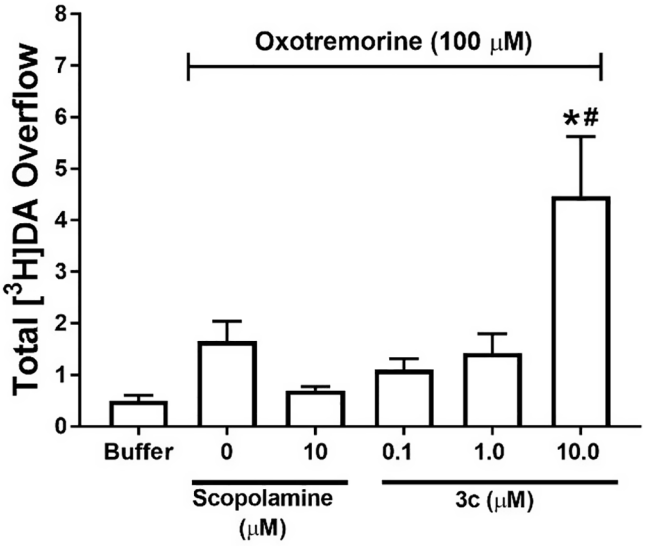

Fig. 3. Compound **3c** increases oxotremorine (100 μM)-evoked [^{3}H]DA overflow from rat striatal slices. A range of concentrations (0.1, 1, and 10 μM) of **3c** were evaluated. Scopolamine (10 μM) was used as the positive control. $^*p < 0.05$ compared to buffer, $^\#p < 0.05$ compared to oxotremorine alone (scopolamine 0 μM), n = 4–10.

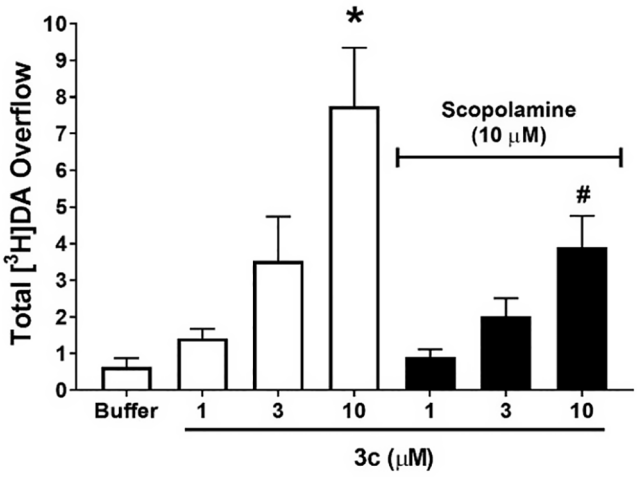

Fig. 4. Scopolamine (10 μM) inhibits **3c**-evoked [^{3}H]DA overflow from superfused rat striatal slices. $^*p < 0.05$ compared to buffer (in the absence of **3c**), $^\#p < 0.05$ compared to **3c** (10 μM) in the absence of scopolamine, n = 6.

slices from KO mice, the current results suggest that oxotremorine increases striatal DA release via stimulation of M_4 and/or M_5 mAChRs, but not via M_3 mAChRs. Based on the results from the KO studies,[40] stimulation of M_3 mAChRs would be expected to decrease DA release. Assuming mAChR modulation of DA release is similar in rats and mice, the lead compound **3c** appears to evoke DA release from rat striatal slices either though an agonist action at M_4 and/or M_5 mAChRs, or through an antagonist action at M_3. In any case, **3c** increases striatal DA release via an agonist action at mAChRs, since this effect is inhibited by scopolamine.

Another important finding from the present study is that the two structural scaffolds provided analogs that exhibit selectivity for M_3 over M_2. Out of the 30 analogs evaluated, 9 analogs (**2d**, **2j**, **2 l**, **2n**, **2o**, **2q**, **3a**, **3b** and **3c**) exhibit relatively high affinity (K_i < 100 nM) at M_3 mAChRs. For these 9 analogs, selectivity at M_3 over M_2 mAChRs was determined in consideration of their potential efficacy in treating COPD. Of note, compound **3b** exhibited 17-fold selectivity for M_3 over M_2 mAChRs. Selectivity between M_3 and M_2 subtypes is important because antagonists at M_3 mAChRs decrease airway smooth muscle contraction and decrease mucus secretion, which would be beneficial in the treatment of COPD; whereas, antagonism at M_2 mAChRs increases acetylcholine release from parasympathetic nerves innervating the airway smooth muscle and submucosal glands, ultimately stimulating M_3 mAChRs and counteracting the beneficial M_3 antagonism produced by therapeutic agents targeting M_3.[41,42] Using the [^{3}H]NMS binding assay, several compounds have been reported previously to be highly potent (low nM range) and selective for M_3 over M_2 mAChRs.[45,46] Specifically, (2*R*)-1-((2*S*,4*R*)-4-hydroxy-1-[3,3,3-tris(4-fluoro-phenyl) propanoyl]-pyrrolidine-2-yl)carbonyl-*N*-(4-piperidinyl-methyl)pyrrolidine-2-carboxamide (compound **14a**) and (2*R*)-*N*-[1-(6-aminopyridin-2-ylmethyl)piperidin-4-yl]-2-[(1*R*)-3,3-difluorocyclopentyl]-2-hydroxy-2-phenylacetamide (compound **A**) exhibit 1600- and 193-fold selectivity, respectively, for M_3 over M_2.[36,43] **14a** and **A** act as M_3 mAChR antagonists as indicated by inhibition of carbachol-induced contraction of the isolated rat tracheal muscle.[36,43] Interestingly, tiotropium and umeclidinium, exhibit only 2 to 3-fold selectivity at M_3 relative to M_2 mAChRs, as indicated from [^{3}H]NMS binding assays.[44–46] Despite, marginal selectivity for M_3, tiotropium and umeclidinium have kinetic selectivity for M_3 and long dissociation half-lifes.[44] Moreover, both compounds are FDA-approved COPD inhalation therapeutics. Thus, the current findings that **3b** has high affinity (K_i = 7.6 nM) and 17-fold selectivity for M_3 over M_2 mAChRs suggest that this compound may have beneficial therapeutic effects over currently available medications for COPD.

In summary, through the synthesis and evaluation of two series of carbamates, **3c** was identified as the most potent (K_i = 1.8 nM) analog interacting at M_5 mAChRs. Although **3c** exhibited 1200-fold higher affinity for M_5 mAChRs compared to compound **1**, **3c** lacked selectivity for M_5 mAChRs. Interestingly, compound **1** inhibited oxotremorine-evoked DA release from rat striatal slices, whereas **3c** augmented oxotremorine-evoked DA release, and moreover, itself increased DA release, indicating that **3c** acts as a mAChR agonist. Future structure activity relationship studies using **3c** as the lead compound will be needed to identify analogs with high affinity and selectivity for M_5. Additionally, **3b** exhibited high affinity and selectivity for M_3 over M_2 mAChRs and may have potential to be developed as a COPD treatment.

Acknowledgment

This work was supported by funding from the National Institute of Health including grants DA 030667 and UL1 TR001998.

References

1. Eglen RM. *Auton Autacoid Pharmacol.* 2006;26:219.
2. Fryer AD, Christopoulos A, Nathanson NM. *Handb Exp Pharmacol.* 2012:208 Chapter 1.
3. Levey AI. *Proc Natl Acad Sci USA.* 1996;93:13541.
4. Digby GJ, Shirey JK, Conn PJ. *Mol Biosyst.* 2010;6:1345.
5. Lebois EP, Bridges TM, Lewis LM, et al. *ACS Chem Neurosci.* 2010;1:104.
6. Jiang S, Li Y, Zhang C, et al. *Neurosci Bull.* 2014;30:295.
7. Fisher A, Pittel Z, Bar-Ner N, et al. *J Mol Neurosci.* 2003;20:349.
8. Barnes PJ. *Thorax.* 1989;44:161.
9. Walker JK, Gainetdinov RR, Feldman DS, et al. *Am J Physiol Lung Cell Mol Physiol.* 2004;386:L312.
10. Chin SJ, Curmowicz AG, Chowdhury BA. *Ann Am Thorac Soc.* 2016;13:173.
11. U.S. Food and Drug Administration. Drugs@FDA. Approval History and Summary Review for Spiriva Respimat NDA 207070 https://www.accessdata.fda.gov/scripts/cder/daf/index.cfm?event=overview.process&applno=021395.
12. Goldenberg MM. *P&T.* 2014;39:112.
13. Yeomans JS. *Handb Exp Pharmacol.* 2012;208:243.
14. Vilaro MT, Palacios JM, Mengod G. *Neurosci Lett.* 1990;114:154.
15. Weiner DM, Levey AL, Brann MR. *Proc Natl Acad Sci USA.* 1990;87:7050.
16. Yasuda RP, Ciesla W, Flores LR, et al. *Mol Pharmacol.* 1993;43:149.
17. Lein ES, Hawrylycz MJ, Ao N, et al. *Nature.* 2007;445:168.
18. Omelchenko N, Sesack SR. *J Comp Neurol.* 2006;494:863.
19. Di Chiara G, Imperato A. *Proc Natl Acad Sci USA.* 1988;85:5274.
20. Chevrette J, Stellar JR, Hesse GW, Markou A. *Pharmacol Biochem Behav.* 2002;71:501.

21. Koob GF, Sanna PP, Bloom FE. *Neuron.* 1998;21:467.
22. Lyness WH, Friedle NM, Moore KE. *Pharmacol Biochem Behav.* 1979;11:553.
23. Steidl S, Miller AD, Blaha CD, Yeomans JS. *PLoS One.* 2011;6:e27538.
24. Wasserman DI, Wang HG, Rashid AJ, Josselyn SA, Yeomans JS. *Eur J Neurosci.* 2013;38:2774.
25. Raffa RB. *J Clin Pharm Ther.* 2009;34:623.
26. Fink-Jensen A, Fedorova I, Wörtwein G, et al. *J Neurosci Res.* 2003;74:91.
27. Thomsen M, Woldbye DP, Wörtwein G, Fink-Jensen A, Wess J, Caine SB. *J Neurosci.* 2005;25:8141.
28. Steidl S, Yeomans JS. *J Pharmacol Exp Ther.* 2009;328:263.
29. Zheng G, Smith AM, Huang X, et al. *J Med Chem.* 2013;56:1693.
30. Prat M, Buil MA, Fernández MD, et al. *Bioorg Med Chem Lett.* 2011;21:3457.
31. Bonner TI, Young AC, Brann MR, Buckley NJ. *Neuron.* 1988;1:403.
32. Lee N-R, Zhang X, Darna M, Dwoskin LP, Zheng G. *Bioorg Med Chem Lett.* 2015;25:5032.
33. [^{3}H]NMS binding assay: [^{3}H]NMS binding assays were performed using 96-well plates. Membrane aliquots containing 10 μg of protein per well for M_1 or M5 mAChRs subtypes, 20 μg of protein per well for M_2 or M_4 mAChRs subtypes, and 3 μg of protein per well for M_3 mAChRs were added to wells containing 1 nM to 100 μM of analog, 0.3 nM [^{3}H]NMS (specific activity 84.2 Ci/mmol; Perkin-Elmer/NEN, Boston, MA) and buffer (50 mM Tris–HCl, pH 7.4) and then incubated for 2 h at 25 °C. Nonspecific binding of [^{3}H]NMS was determined in the presence of 1 μM atropine. Reactions were terminated by rapid filtration onto GF/B filters using a Filtermate harvester (PerkinElmer Life and Analytical Sciences, Boston, MA) and washed three times with 50 mM Tris–HCl buffer (pH 7.4). Subsequently, 40 μL of MicroScint 20 (PerkinElmer Life and Analytical Sciences, Waltham, MA) was added to each well and radioactivity bound determined using liquid scintillation spectrometry.
34. Cheng Y, Prusoff WH. *Biochem Pharmacol.* 1973;22:3099.
35. Moriya H, Takagi Y, Hayashi M, Tani T, Hirotsu I. *Life Sci.* 1999;64:2351.
36. Hirose H, Aoki I, Kimura T, et al. *J Pharmacol Exp Ther.* 2001;297:790.
37. Naito R, Yonetoku Y, Okamoto Y, Toyoshima A, Ikeda K, Takeuchi M. *J Med Chem.* 2005;48:6597.
38. [^{3}H]DA release assay: Rat striata were dissested and sliced (500 μm, 4-6 mg). Striatal slices were incubated in Krebs' buffer (108 mM NaCl, 4.7 mM KCl, 1.2 mM $MgCl_2$, 1 mM NaH_2PO_4, 1.3 mM $CaCl_2$, 11.1 mM glucose, 25 mM $NaHCO_3$, 0.11 mM L-ascorbic acid and 0.004 disodium EDTA, pH7.4) for 60 min at 34 °C. During the latter 30 min of the incubation, [^{3}H]DA (0.1 μM) was added to the incubation buffer. Each striatal slice was placed in a superfusion chamber after incubation, and then superfused (0.6 mL/min) with Krebs' buffer for 60 min in the presence of nomifensine (a DA transporter inhibitor; 10 μM) and pargyline (a monoamine oxidase inhibitor; 10 μM). Samples were collected every 5 min for a total of 75 min. Samples collected during the first 15 min were used to determine [^{3}H]DA basal outflow. Samples were collected for 35 min in the absence or presence of scopolamine or **3c**, followed by 25 min in absence or presence of oxotremorine (100 μM) in the superfusion buffer. [^{3}H]DA overflow was determined as the summation of radioactivity in superfusate samples during exposure to compound following the substraction of basal outflow across the same time period. Radioactivity was determined using liquid scintillation spectroscopy.
39. Barocelli E, Ballabeni V, Bertoni S, et al. *Bioorg Med Chem Lett.* 2000;67:717.
40. Zhang W, Yamada M, Gomeza J, Basile AS, Wess J. *J Neurosci.* 2002;22:6327.
41. Buels SK, Fryer DA. *Handb Exp Pharmacol.* 2012;208:317.
42. Gosens R, Zaagsma J, Meurs H, Halayko AJ. *Respir Res.* 2006;7:73.
43. Sagara Y, Sagara T, Uchiyama M, et al. *J Med Chem.* 2006;49:5653.
44. Sykes DA, Dowling MR, Leighton-Davies J, et al. *J Pharmacol Exp Ther.* 2012;343:520.
45. Salmon M, Luttmann MA, Foley JJ, et al. *J Pharmacol Exp Ther.* 2013;345:260.
46. Dowling MR, Charlton SJ. *Br J Pharmacol.* 2006;148:927.